

Quantum interference control of current in semiconductors: Universal scaling and polarization effects

M. Sheik-Bahae*

Department of Physics and Astronomy, University of New Mexico, Albuquerque, New Mexico 87131

(Received 2 July 1999)

Quantum interference control of current in bulk semiconductors is analyzed using a simple three-band model. Universal scaling rules and polarization dependence are analytically derived. [S0163-1829(99)50840-0]

Quantum interference control (QUIC) of current in semiconductors is a subject of current interest dealing with the manipulation of the magnitude and the direction of a photo-current.¹⁻⁴ It is an example of a class of phenomena involving quantum interference between optical transitions that have been studied in atomic media.⁵⁻⁷ In all cases, interference between single-photon absorption (SPA) and two-photon absorption (TPA) produces directional photoelectrons in the continuum of conduction band states. The directionality of the photogenerated electrons results from the fact that the two pairs of initial and final states involved in the single- and two-photon transitions are degenerate but contain different parity. Device applications based on QUIC in semiconductors have now been proposed, including the generation of short (single cycle) bursts of terahertz frequency radiation.^{3,8,9}

A calculation of the QUIC current density tensor J_{ijkl} in bulk semiconductors was given by Atanasov *et al.*⁴ for GaAs using a numerical model which uses a full band structure of GaAs within the local density approximation. Khurgin⁸ employed a simple parabolic band structure to show that QUIC and third-order optical rectification are the “real” and “virtual” manifestations of the same nonlinear process. In this paper, a three-band model will be presented that, in analytical form, describes the QUIC scaling as well as its polarization dependence. Simple theoretical models leading to analytical solutions allow for a generality that is descriptive of a large class of materials. A simple model also provides a clear physical picture that is often difficult to extract from numerical treatments.

The system studied here is a zinc-blende semiconductor characterized by a conduction band and two valence bands in Kane’s theory.¹⁰ The two valence bands are a heavy-hole (hh) and a light-hole (lh) band as depicted in Fig. 1. The starting formalism is described in Refs. 11 and 12 where initial (valence) and final (conduction) states are taken as dressed Bloch functions where the acceleration of the electrons and holes are taken into account by considering the first order (i.e., time-dependent) Stark shift of the energy states due to the applied fields:

$$\psi_{c,v}(\mathbf{k}, \mathbf{r}, t) = u_{c,v}(\mathbf{k}, r) \exp \left[i\mathbf{k} \cdot \mathbf{r} - i\omega_{c,v}(k)t + \frac{ie}{m_{c,v}} \int_0^t \mathbf{k} \cdot \mathbf{A}(\tau) d\tau \right], \quad (1)$$

where $E_{c,v}^0(k) = \hbar\omega_{c,v}(k)$ is the stationary energy eigenvalue of each band with effective masses m_c and m_v ($v = \text{hh}$ or lh). The total vector potential $\mathbf{A}(\tau)$ contains two harmonic fields at ω and 2ω specified by their amplitude A_j , phase ϕ_j , and polarization unit vector \mathbf{a}_j ($j = 1, 2$) as follows:

$$\mathbf{A} = \mathbf{a}_1 A_1 \cos(\omega t + \phi_1) + \mathbf{a}_2 A_2 \cos(2\omega t + \phi_2). \quad (2)$$

The electron-hole generation rate is calculated using first-order perturbation theory,

$$S = \frac{i}{\hbar} \int_{-\infty}^t dt' \int d^3r \psi_c^*(k, r, t') H_{\text{int}} \psi_v(k', r, t'), \quad (3)$$

where $H_{\text{int}} = -(e/m_0 c) \mathbf{A} \cdot \mathbf{p}$ is the interaction Hamiltonian. The momentum distribution of the photogenerated electrons is obtained by evaluating the transition rate for single and two-photon process as a function of Euler’s angles θ and ϕ in the k space:

$$W(\theta, \phi) = \lim_{t \rightarrow \infty} \int \frac{\sin(\theta) k^2 dk}{(2\pi)^3} \frac{d}{dt} |S|^2. \quad (4)$$

Note that the absolute magnitude of the electron-hole quasi-momentum $|k|$ is determined from the energy conservation relation [$E_c^0(k) - E_v^0(k) = 2\hbar\omega$] contained in Eq. (3). Assuming parabolic bands, we have $E_c^0 = E_g + \hbar^2 k^2 / 2m_c$ and $E_v^0 = \hbar^2 k^2 / 2m_v$, where E_g is the direct band gap energy. Using $k \cdot p$ theory, we make the valid approximations for states near $k = 0$ that $m_c = -m_{\text{lh}} \approx m_0 E_g / E_p$ and $m_{\text{hh}} \approx m_0$, where m_0 is the bare electron mass, and $E_p \approx 21$ eV is the Kane

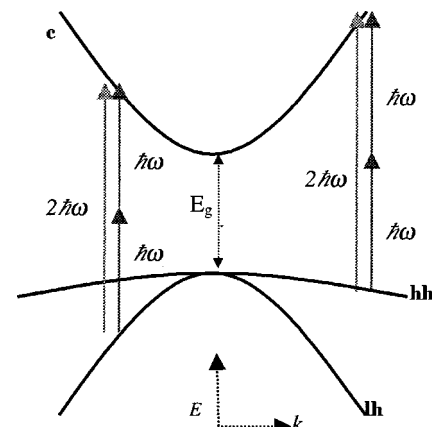


FIG. 1. The Kane three-band model.

TABLE I. The functional form of the photocarrier distribution in k space.

		F^α	F^β	$F^{\alpha\beta}$
lh- c	$a_1 \parallel \mathbf{z}$	$\left(\frac{3}{4\pi}\right) \sin(\theta) \cos^2(\theta)$	$\left(\frac{5}{4\pi}\right) \sin(\theta) \cos^4(\theta)$	$\left(\frac{\sqrt{15}}{4\pi}\right) \sin(\theta) \cos^3(\theta)$
	$a_2 \parallel \mathbf{z}$			
	$a_1 \parallel \mathbf{z}$	$\left(\frac{3}{4\pi}\right) \sin^3(\theta) \sin^2(\phi)$	$\left(\frac{5}{4\pi}\right) \sin(\theta) \cos^4(\theta)$	$\left(\frac{\sqrt{15}}{4\pi}\right) \sin^2(\theta) \cos^2(\theta) \sin(\phi)$
	$a_2 \parallel \mathbf{y}$			
hh- c	$a_1 \parallel \mathbf{z}$	$\left(\frac{3}{4\pi}\right) \frac{\sin^3(\theta)}{2}$	$\left(\frac{15}{4\pi}\right) \frac{\sin^3(\theta) \cos^2(\theta)}{2}$	$\left(\frac{\sqrt{45}}{4\pi}\right) \frac{\sin^3(\theta) \cos(\theta)}{2}$
	$a_2 \parallel \mathbf{z}$			
	$a_1 \parallel \mathbf{z}$	$\left(\frac{3}{4\pi}\right) \frac{\sin(\theta)}{2}$	$\left(\frac{15}{4\pi}\right) \frac{\sin^3(\theta) \cos^2(\theta)}{2}$	$-\left(\frac{\sqrt{45}}{4\pi}\right) \frac{\sin^2(\theta) \cos^2(\theta) \sin(\phi)}{2}$
	$a_2 \parallel \mathbf{y}$	$\times [\cos^2(\theta) \sin^2(\phi) + \cos^2(\phi)]$		

energy which is material independent for most semiconductors. In the Kane band structure, the conduction band is s type and the valence bands are p type. The wave functions of the valence bands can be written as a superposition of the band-edge Bloch wave functions $|X\rangle$, $|Y\rangle$, and $|Z\rangle$. Specifically, the hh valence band is of $|X \pm iY\rangle$ form while the lh band is a superposition of $|X \pm iY\rangle$ and $|Z\rangle$ wave functions. Without loss of generality, taking $\mathbf{k} \parallel \mathbf{z}$ causes no $k \cdot p$ coupling between the conduction and hh-valence bands. The absence of $k \cdot p$ coupling in the hh- c interaction is the reason why the mass of the hh valence band is the same as the bare electron mass. For optical transitions, these symmetry arguments allow us to take $\mathbf{k} \parallel \mathbf{p}_{cv}$ for the lh- c , and $\mathbf{k} \perp \mathbf{p}_{cv}$ for the hh- c , where \mathbf{p}_{cv} is the interband momentum matrix element.¹⁰ The k space symmetry relations thus determine the momentum distribution of the electron-hole pairs $W(\theta, \phi)$ and hence the polarization dependence of the photocurrent. Evaluation of Eq. (4), retaining only the lowest order terms in A_1 and A_2 gives

$$W(\theta, \phi) = \frac{1}{2\hbar\omega} [\alpha I_2 F^\alpha(\theta, \phi) + \beta I_1^2 F^\beta(\theta, \phi) + 2\sqrt{\alpha I_2 \beta I_1^2} F^{\alpha\beta}(\theta, \phi) \sin(2\theta_1 - \theta_2)], \quad (5)$$

where $I_1 = [n(\omega) \varepsilon_0 \omega^2 / 2c] A_1^2$ and $I_2 = [2n(2\omega) \varepsilon_0 \omega^2 / c] A_2^2$ denote the irradiance of the two beams, and α and β are the SPA and TPA coefficients at 2ω and ω , respectively. These coefficients are

$$\beta = K \frac{\sqrt{E_p}}{n(\omega)^2 E_g^3} \frac{(2x-1)^{3/2}}{(2x)^5}$$

and

$$\alpha = A \frac{E_g}{n(2\omega) \sqrt{E_p}} \frac{(2x-1)^{1/2}}{2x}, \quad (6)$$

with

$$K = \frac{2^9 (3 + \sqrt{2}) \pi}{15} \frac{1}{(4\pi\varepsilon_0)^2} \frac{e^4}{\sqrt{m_0 c^2}}$$

and

$$A = \frac{2 + 4\sqrt{2}}{3} \frac{e^2 \sqrt{m_0}}{4\pi\varepsilon_0 \hbar^2 c}. \quad (7)$$

The absorption coefficients α and β are identical to those derived for two-band models,^{12,13} except that numerical prefactors in K and A used here are modified to include the presence of an additional valence band. The spectral dependence is contained in functions involving $x = \hbar\omega/E_g$. The calculated angular distribution functions F^α , F^β , and $F^{\alpha\beta}$ corresponding to SPA, TPA, and the interference term, respectively, are listed in Table I. F^α and F^β are normalized such that $\iint F^j d\theta d\phi = 1$, where $j = \alpha, \beta$. We note that $\iint F^{\alpha\beta} d\theta d\phi = 0$, indicating the fact that the interference does not produce additional carriers by itself, but only alters (i.e., destroys the symmetry of) the momentum distribution of the photogenerated electron-hole population. To illustrate this, examples of three-dimensional electron distributions $W(\theta, \phi)$ resulting from lh- c and hh- c transitions are plotted in Fig. 2, assuming $\alpha I_2 = 4\beta I_1^2$ and co-polarized beams. Note that there is asymmetry in the momentum distribution only along the polarization direction. Furthermore, varying the relative phase ($\Delta\phi$) controls the direction of injected e - h populations. The transition lh- c gives a much more pronounced k space anisotropy compared to hh- c although the phase dependence is identical. Dramatically different results are obtained for cross-polarized beams as depicted in Fig. 3 for $\Delta\phi = (2m+1)\pi/2$ ($m = \text{integer}$). The first feature is that the anisotropy in the distribution is obtained only along the polarization direction of the 2ω beam. Second, the anisotropy introduced by the hh- c and lh- c transitions almost cancel, leading to a nearly symmetric total distribution.

The instantaneous rate of the current injection produced due to the QUIC process along a direction \hat{i} in the presence

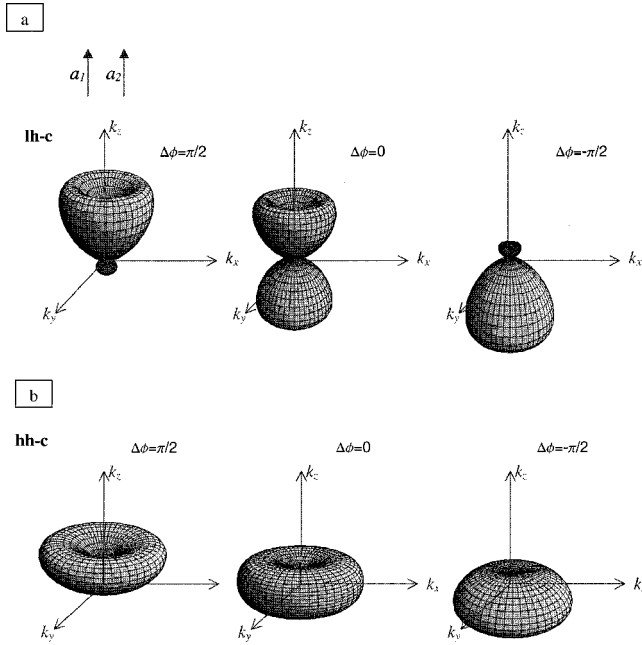


FIG. 2. Momentum distribution of the photocarriers assuming co-polarized beams for (a) lh-c transitions and (b) hh-c transition calculated for various values of $\Delta\phi$ at $\alpha I_2 = 4\beta I_1^2$.

of two beams with irradiances I_1 and I_2 having photon energies $\hbar\omega$ and $2\hbar\omega$ and polarization directions \hat{l} and \hat{k} , respectively, is

$$\mathbf{j}_{ikll}^{e,h} = e \nu_{e,h} \langle W_i \rangle, \quad (8)$$

where $\langle W_i \rangle$ denotes the projected sum of $W(\theta, \phi)$ along the \hat{i} direction and $\nu_{e,h} = \sqrt{2(2\hbar\omega - E_g)m_{c,v}/m_{c,v}^2}$ is photo-generated electron or hole velocity. It is important to note that in the simple static lattice model assumed here, the recoil momentum is absorbed by “infinitely” heavy ions.

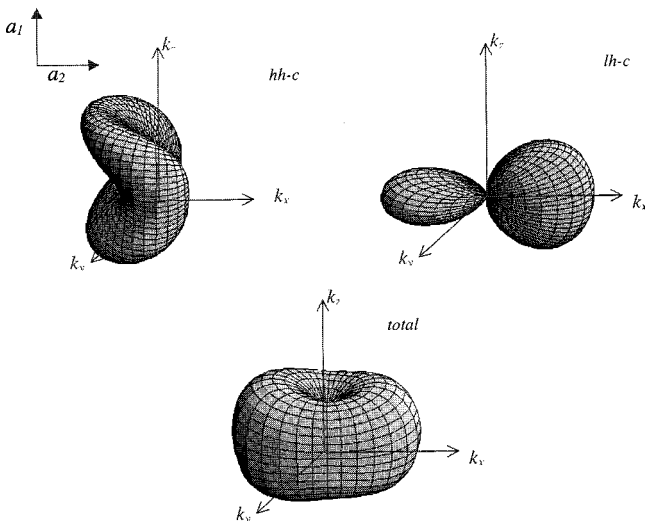


FIG. 3. Momentum distribution of the photocarriers for the lh-c transition, hh-c transition, and the sum of the two distributions calculated for cross-polarized beams and the condition $\alpha I_2 = 4\beta I_1^2$.

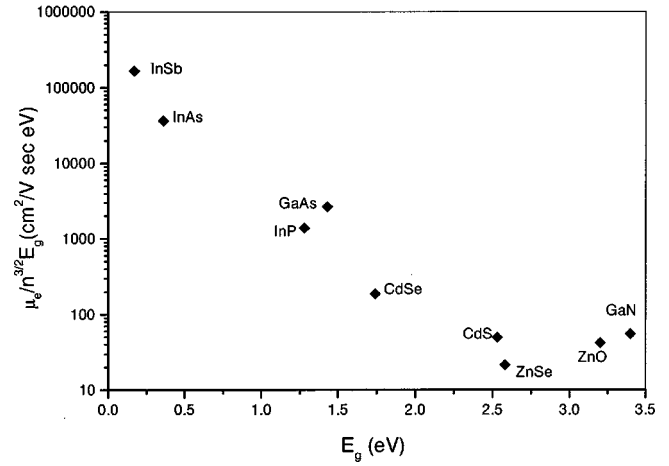


FIG. 4. Band-gap scaling of the macroscopic injected current density for various direct gap semiconductors.

Evaluating Eq. (8) for electrons and summing the contributions from lh and hh valence bands leads to an instantaneous current density rate,

$$\mathbf{j}_{ikll}^e(t) = \frac{Be}{\sqrt{m_0}} \frac{\sqrt{E_p}}{E_g} \frac{\sqrt{2x-1}}{x} \times \sqrt{\alpha\beta} I_2(t) I_1^2(t) \sin(2\phi_1 - \phi_2) Y_{ijkl}, \quad (9)$$

where $B \approx 0.6$ is a numerical constant. The tensor properties are contained in the dimensionless Y_{ijkl} parameter given in Table II. The predicted polarization dependence is in agreement with experimental observations in GaAs.³ As pointed out by Hache *et al.*,³ the macroscopic current density will be strongly influenced by the rate at which the injected $e-h$ distribution is randomized due to phonon scattering. Ignoring recombination and diffusion, the macroscopic current density (\bar{J}) evolves according to

$$\dot{\bar{J}} + \frac{\bar{J}}{\tau_m} = \mathbf{j}_{ikll}^{e,h}, \quad (10)$$

where τ_m denotes the momentum relaxation time. The average current density over a time interval $T \gg \tau_m$, and assuming a temporally square pulse of duration t_p , is then obtained from Eq. (10):

$$\langle \bar{J} \rangle \approx \gamma \frac{t_p}{T} I_{01} I_{02}^{1/2} \sin \Delta\phi, \quad (11)$$

with γ given by

$$\gamma = \sqrt{\frac{m_0}{E_p}} \mu_e \sqrt{\alpha\beta} \frac{\sqrt{2x-1}}{x} Y_{ijkl}, \quad (12)$$

where $\mu_e = e\tau_m/m_c$ is the carrier (here electronic) mobility. In an experiment performed with modelocked laser pulses, T can be taken as the pulse train period. The result in Eq. (12) indicates that the critical material parameter for obtaining strong QUIC signals is the $\mu_e \sqrt{\alpha\beta}$ product. The material scaling can be found by substituting the known band-gap

TABLE II. The tensor coefficient of the injected current density rate for both band pairs.

	lh-c	hh-c	Total
Y_{xxxx}	$\frac{3}{2\sqrt{2}+3}$	$\frac{2\sqrt{2}}{2\sqrt{2}+3}$	1
Y_{yxxx}	0	0	0
Y_{xxyy}	$\frac{1}{2\sqrt{2}+3}$	$\frac{-\sqrt{2}}{2\sqrt{2}+3}$	-0.07
Y_{yyyy}	0	0	0

dependence of α , β , and μ_e . Incorporating the scaling of SPA and TPA given in Eq. (6), we arrive at the following scaling relation for γ :

$$\gamma \propto \frac{\mu_e}{n^{3/2} E_g}, \quad (13)$$

where we have ignored the dispersion of the linear refractive index. Using the known electron mobility and refractive index,¹⁴ we plot in Fig. 4 the parameter γ for a number of III-V and II-VI semiconductors. Since electron mobility

makes the strongest contribution, the semiconductors such InAs and InSb have the best potential for generating large coherent currents and bursts of terahertz frequency radiation.

Additional material parameters can play a role in the scaling of the total macroscopic current depending on the experimental arrangement. In contactless experiments (i.e., in terahertz detection⁹) the depth of the coherent current will be determined by either the optical absorption depth $l_a = \alpha^{-1}(2\omega)$ or coherence length of the two beams $l_c = \lambda/[n(2\omega) - n(\omega)]$.³ In planar metal-semiconductor-metal structures, however, the effective current depth can be determined by the mean free path between momentum randomizing collisions ($l_m = v_{e,h} \tau_m \approx 10-500$ nm) if carriers are generated within a distance l_m of the electrode. Clearly, the latter effect will make the mobility dependence of the scaling parameter even stronger than that given by Eq. (13), although the relative position of the points in Fig. 4 should remain the same.

In conclusion, a three-band model describes the magnitude, band-gap scaling, and the polarization dependence of coherent current control in semiconductors. Materials with high current injection efficiencies are identified using the derived scaling law.

The author gratefully acknowledges support from NSF CAREER (ECS-9625532).

*Electronic address: msbahae@astro.phys.unm.edu

¹A. Hache, Y. Kostoulas, R. Atanasov, J. L. P. Hughes, J. E. Sipe, and H. M. van Driel, *Phys. Rev. Lett.* **78**, 306 (1997).

²E. Dupont, P. B. Corkum, H. C. Liu, M. Buchanan, and Z. R. Wasilewski, *Phys. Rev. Lett.* **74**, 3596 (1995).

³A. Hache, J. E. Sipe, and H. M. van Driel, *IEEE J. Quantum Electron.* **34**, 1144 (1998).

⁴R. Atanasov, A. Hache, J. L. P. Hughes, H. M. van Driel, and J. E. Sipe, *Phys. Rev. Lett.* **76**, 1703 (1996).

⁵E. A. Manykin and A. M. Afanas'ev, *Zh. Eksp. Teor. Fiz.* **52**, 1246 (1967) [*Sov. Phys. JETP* **25**, 828 (1967)].

⁶B. Y. Zeldovich and A. N. Chudinov, *Pis'ma Zh. Eksp. Teor. Fiz.* **50**, 405 (1989) [*JETP Lett.* **50**, 439 (1989)].

⁷Y. Y. Yin, C. Chen, D. S. Elliott, and A. V. Smith, *Phys. Rev. Lett.* **69**, 2353 (1992).

⁸J. B. Khurgin, *J. Nonlinear Opt. Phys. Mater.* **4**, 163 (1995).

⁹D. Cote, J. M. Fraser, H. M. van Driel, T. Weinacht, M. DeCamp, and P. H. Bucksbaum, *Quantum Electronics and Laser Science Conference*, OSA Technical Digest (Optical Society of America, Washington, D.C., 1999), pp. 220-221.

¹⁰E. O. Kane, *J. Phys. Chem. Solids* **1**, 249-261 (1957).

¹¹H. D. Jones and H. R. Reiss, *Phys. Rev. B* **16**, 2466 (1977).

¹²M. Sheik-Bahae, D. C. Hutchings, D. J. Hagan, and E. W. Van Stryland, *IEEE J. Quantum Electron.* **27**, 1296 (1991).

¹³B. S. Wherrett, *J. Opt. Soc. Am. B* **1**, 67 (1984).

¹⁴J. I. Pankove, *Optical Processes in Semiconductors* (Dover, New York, 1971).